NME1701
pp: 1-22 (col.fig.: Nil)
PROD. TYPE: COM
ED: RM
PAGN: Usha.K – SCAN: Agnes

INTERNATIONAL JOURNAL FOR NUMERICAL METHODS IN ENGINEERING
Int. J. Numer. Meth. Engng (in press)
Published online in Wiley InterScience (www.interscience.wiley.com). DOI: 10.1002/nme.1701

A constrained reproducing kernel particle formulation for shear deformable shell in Cartesian coordinates

Jiun-Shyan Chen[1,*,†] Dongdong Wang[2,‡]

[1]*Department of Civil and Environmental Engineering, University of California, Los Angeles, CA 90095-1593, U.S.A.*
[2]*Department of Civil Engineering, Xiamen University, Xiamen, Fujian 361005, People's Republic of China*

SUMMARY

The meshfree approximation functions for shell analysis to date are formulated using parametric coordinates, and this parametric description of shell kinematics limits the applications only to shell structures with simple geometries. On the other hand, construction of moving least square or reproducing kernel (RK) approximation on shell surface using Cartesian coordinates leads to a singular system when RK basis functions and shell surface function are linearly dependent. In this study, a constrained RK approximation formulated under Cartesian coordinate for approximation of shell kinematics in arbitrary shell geometry is proposed. Two methods, the dummy node approach and the pseudo-inverse method, are presented. Further, stabilization of nodal integration for solving shear deformable shell is introduced. The performance of present formulation is demonstrated in several benchmark problems. Copyright © 2006 John Wiley & Sons, Ltd.

KEY WORDS: constrained reproducing kernel approximation; shear deformable shell; stabilized conforming nodal integration

1. INTRODUCTION

The meshfree shell formulations [1, 2] proposed to date employed parametric coordinates in the construction of the approximation functions. Under the framework of element-free Galerkin method [3, 4], it was demonstrated in References [1, 5] that the C^1 continuity required in the solution of Kirchhoff plates and shells can be easily obtained using moving least square

*Correspondence to: Jiun-Shyan Chen, Department of Civil and Environmental Engineering, University of California, Los Angeles, CA 90095-1593, U.S.A.
†E-mail: jschen@seas.ucla.edu
‡E-mail: ddwang@xmu.edu.cn

Contract/grant sponsor: Research Initiation Fund

Received 17 September 2005
Revised 9 February 2006
Accepted 9 February 2006

(MLS) approximation in parametric coordinates. In Reference [6], 3D meshfree method was directly adopted to analyse shell structures without employing shell theory which needs more computational effort. In Reference [2], a shear deformable meshfree shell formation was introduced by employing a parametric mapping technique, where the MLS approximation was constructed using the mapped convected coordinates. In order to avoid shear and membrane locking, bi-cubic complete polynomial basis in convected parametric coordinates were adopted for the approximation of kinematic variables. However, by the employment of parametric coordinates, neither MLS nor reproducing kernel (RK) approximations can be constructed when the shell geometry is described by multiple parametric domains. On the other hand, formulating MLS or RK approximation using Cartesian coordinates leads to a singular moment matrix in the construction of shape functions when the reproducing equations and the equation describing shell surface are linearly dependent.

To resolve the difficulty in formulating MLS/RK approximation using Cartesian coordinates, we propose a constrained RK approximation for meshfree analysis of shell structures. To avoid the singular moment matrix, two methods are proposed. In the first approach, a set of dummy nodes perturbed from the physical nodes on the shell surface are introduced. By formulating RK approximation using the physical and dummy nodes, in conjunction with a static condensation procedure by taking the limit of the distance between the physical and dummy nodes, constrained Cartesian RK shape functions are obtained. The second approach is introduced by realizing that the right-hand side vector of the reproducing equations is orthogonal to the null space of moment matrix. This allows an employment of a pseudo-inverse formulation to solve reproducing equations that are linearly dependent in the global Cartesian coordinates.

This paper is organized as follows. The singularity in the Cartesian RK approximation on constrained shell surface is illustrated in Section 2. In Section 3, two constrained Cartesian RK methods are given to deal with this singularity, one using a dummy node technique and the other employing a pseudo-inverse method. Representation of shell geometry using constrained RK approximation is also shown. In Section 4, a meshfree shell formulation using the proposed constrained Cartesian RK approximations is presented. A stabilization of nodal integration for curved shell surface is discussed in Section 5. Numerical examples are given in Section 6 and conclusions are drawn in Section 7.

2. SINGULARITY IN CARTESIAN RK APPROXIMATION ON SHELL SURFACE

Consider a shell structure with domain $\Omega \subset S$, where S is a surface described by a surface function:

$$S = \{\mathbf{x} : F(\mathbf{x}) = 0\} \tag{1}$$

Let the problem domain Ω be discretized by a set of NP particles $\{\mathbf{x}_1, \mathbf{x}_2, \ldots, \mathbf{x}_{\mathrm{NP}}\}$, and $\mathbf{x}_I \in S$. The RK approximation [7–9] of a function $u_i(\mathbf{x})$ is expressed as

$$u_i(\mathbf{x}) = \sum_{I=1}^{\mathrm{NP}} \Phi_a(\mathbf{x}; \mathbf{x} - \mathbf{x}_I) d_{Ii} \tag{2}$$

NME1701

where Φ_a and d_{Ii} are the shape functions and nodal coefficients associated with node I. In the RK approximation, the shape function Φ_a is expressed as

$$\Phi_a(\mathbf{x};\mathbf{x}-\mathbf{x}_I)=\sum_{i+j+k=0}^{n}(x-x_I)^i(y-y_I)^j(z-z_I)^k b_{ijk}(\mathbf{x})\phi_a(\mathbf{x}-\mathbf{x}_I)$$

$$\equiv\sum_{i+j+k=0}^{n}h_{ijk}(\mathbf{x}-\mathbf{x}_I)b_{ijk}(\mathbf{x})\phi_a(\mathbf{x}-\mathbf{x}_I) \tag{3}$$

where $h_{ijk}(\mathbf{x})=x^i y^j z^k$ are monomial basis functions, and $\phi_a(\mathbf{x}-\mathbf{x}_I)$ is the kernel function with compact support of measure a centered at $\mathbf{x}_I$.

To obtain the coefficients $b_{ijk}(\mathbf{x})$ in Equation (3), the following nth-order reproducing conditions are imposed:

$$\sum_{I=1}^{\mathrm{NP}}\Phi_a(\mathbf{x};\mathbf{x}-\mathbf{x}_I)h_{ijk}(\mathbf{x}_I)=h_{ijk}(\mathbf{x}),\quad 0\leqslant i+j+k\leqslant n \tag{4}$$

Equation (4) can be recast as

$$\mathbf{M}(\mathbf{x})\mathbf{b}(\mathbf{x})=\mathbf{H}(\mathbf{0}) \tag{5}$$

where

$$\mathbf{M}(\mathbf{x})=\sum_{I=1}^{\mathrm{NP}}\mathbf{H}(\mathbf{x}-\mathbf{x}_I)\mathbf{H}^{\mathrm{T}}(\mathbf{x}-\mathbf{x}_I)\phi_a(\mathbf{x}-\mathbf{x}_I) \tag{6}$$

$$\mathbf{H}^{\mathrm{T}}(\mathbf{x}-\mathbf{x}_I)=[1\quad x-x_I\quad y_2-y_I\quad z-z_I\quad (x-x_I)^2\quad \cdots\quad (z-z_I)^n] \tag{7}$$

If the shell surface can be expressed by the linear combination of basis functions used in Equation (3), we have:

$$F(\mathbf{x})=\sum_{i+j+k=0}^{n}a_{ijk}h_{ijk}(\mathbf{x}-\mathbf{x}_I)=0 \tag{8}$$

When Equation (8) is met, the RK conditions in Equation (4) are clearly linearly dependent, and this results in a singular moment matrix $\mathbf{M}(\mathbf{x})$.

3. CONSTRAINED RK APPROXIMATION ON SHELL SURFACE

Two approaches are proposed in this section to resolve the singularity issue in the Cartesian RK approximation.

3.1. Dummy node method

Let the shell surface be discretized by NP 'physical' nodes $\{x_I, y_I, z_I\}_{I=1}^{\mathrm{NP}}$, as shown in Figure 1. A layer of 'dummy' nodes $\{x_{I+\mathrm{NP}}, y_{I+\mathrm{NP}}, z_{I+\mathrm{NP}}\}_{I=1}^{\mathrm{NP}}$ are created with a perturbed distance

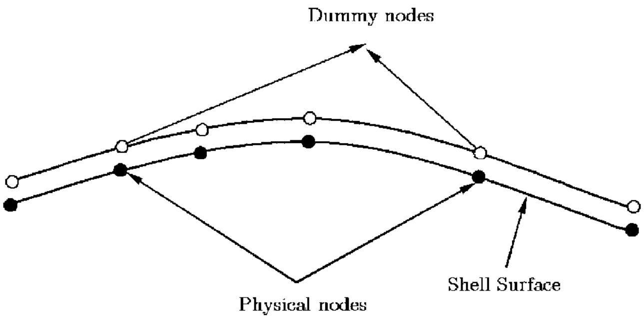

Figure 1. Dummy node approach.

vector $\mathbf{t} = \{t_1, t_2, t_3\}$, $F(\mathbf{x}_I + \mathbf{t}) \neq 0$, $1 \leqslant I \leqslant \mathrm{NP}$, from the physical nodes as

$$\begin{aligned} x_{\mathrm{NP}+I} &= x_I + t_1 \\ y_{\mathrm{NP}+I} &= y_I + t_2 \\ z_{\mathrm{NP}+I} &= z_I + t_3 \end{aligned} \tag{9}$$

The moment matrix $\mathbf{M}$ associated with the RK approximation using both sets of nodes $\{x_I, y_I, z_I\}_{I=1}^{2\mathrm{NP}}$ can be expressed in the following form:

$$\mathbf{M}(\mathbf{x}, \mathbf{t}) = \underbrace{\overbrace{\mathbf{M}_1(\mathbf{x})}^{\text{possibly singular}} - \mathbf{M}_2(\mathbf{x}, \mathbf{t})}_{\text{nonsingular}} \tag{10}$$

where

$$\mathbf{M}_1(\mathbf{x}) = \sum_{I=1}^{\mathrm{NP}} 2\phi_a(\mathbf{x} - \mathbf{x}_I) \begin{pmatrix} 1 & (x-x_I) & (y-y_I) & (z-z_I) \\ (x-x_I) & (x-x_I)^2 & (x-x_I)(y-y_I) & (x-x_I)(z-z_I) \\ (y-y_I) & (x-x_I)(y-y_I) & (y-y_I)^2 & (y-y_I)(z-z_I) \\ (z-z_I) & (z-z_I)(x-x_I) & (z-z_I)(y-y_I) & (z-z_I)^2 \end{pmatrix} \tag{11}$$

$$\mathbf{M}_2(\mathbf{x}, \mathbf{t}) = \sum_{I=1}^{\mathrm{NP}} \phi_a(\mathbf{x} - \mathbf{x}_I) \begin{pmatrix} 0 & t_1 & t_2 & t_3 \\ t_1 & [2t_1(x-x_I) - t_1^2] & \begin{matrix}[t_1(y-y_I) + \\ t_2(x-x_I) - t_1 t_2]\end{matrix} & \begin{matrix}[t_1(z-z_I) + \\ t_3(x-x_I) - t_1 t_3]\end{matrix} \\ t_2 & \begin{matrix}[t_1(y-y_I) + \\ t_2(x-x_I) - t_1 t_2]\end{matrix} & [2t_2(y-y_I) - t_2^2] & \begin{matrix}[t_2(z-z_I) + \\ t_3(y-y_I) - t_2 t_3]\end{matrix} \\ t_3 & \begin{matrix}[t_1(z-z_I) + \\ t_3(x-x_I) - t_1 t_3]\end{matrix} & \begin{matrix}[t_2(z-z_I) + \\ t_3(y-y_I) - t_2 t_3]\end{matrix} & [2t_3(z-z_I) - t_3^2] \end{pmatrix} \tag{12}$$

By the addition of the dummy nodes, the moment matrix $\mathbf{M}$ in Equation (10) can be shown to be nonsingular due to the second term on the R.H.S. of Equation (10). The resulting NP pairs of RK shape functions can be expressed as follows:

$$\Phi_a(\mathbf{x};\mathbf{x}-\mathbf{x}_I)=\mathbf{H}^{\mathrm{T}}(\mathbf{0})\mathbf{M}^{-1}(\mathbf{x})\mathbf{H}(\mathbf{x}-\mathbf{x}_I)\phi_a(\mathbf{x}-\mathbf{x}_I)\equiv\Psi_I^1(\mathbf{x}) \tag{13}$$

$$\Phi_a(\mathbf{x};\mathbf{x}-\mathbf{x}_{I+\mathrm{NP}})=\hat{\mathbf{H}}^{\mathrm{T}}(\mathbf{0})\mathbf{M}^{-1}(\mathbf{x})\hat{\mathbf{H}}(\mathbf{x}-\mathbf{x}_I)\phi_a(\mathbf{x}-\mathbf{x}_I)\equiv\Psi_I^2(\mathbf{x}) \tag{14}$$

where $1\leqslant I\leqslant \mathrm{NP}$ and

$$\mathbf{H}(\mathbf{x}-\mathbf{x}_I)=\begin{bmatrix}1\\ x-x_I\\ y-y_I\\ z-z_I\end{bmatrix},\quad \hat{\mathbf{H}}(\mathbf{x}-\mathbf{x}_I)=\begin{bmatrix}1\\ x-x_I-t_1\\ y-y_I-t_2\\ z-z_I-t_3\end{bmatrix} \tag{15}$$

Note that Equations (13) and (14) satisfy the following reproducing conditions:

$$\begin{aligned}\sum_{I=1}^{2\mathrm{NP}}\Phi_a(\mathbf{x};\mathbf{x}-\mathbf{x}_I)&=1\\ \sum_{I=1}^{2\mathrm{NP}}\Phi_a(\mathbf{x};\mathbf{x}-\mathbf{x}_I)x_I&=x\\ \sum_{I=1}^{2\mathrm{NP}}\Phi_a(\mathbf{x};\mathbf{x}-\mathbf{x}_I)y_I&=y\\ \sum_{I=1}^{2\mathrm{NP}}\Phi_a(\mathbf{x};\mathbf{x}-\mathbf{x}_I)z_I&=z\end{aligned} \tag{16}$$

By letting the perturbed distance $\mathbf{t}\to\mathbf{0}$, we have $(x,y)_{I+\mathrm{NP}}\to(x,y)_I$, and Equation (16) reduces to

$$\begin{aligned}\sum_{I=1}^{\mathrm{NP}}[\Psi_I^1(\mathbf{x})+\Psi_I^2(\mathbf{x})]&=\sum_{I=1}^{\mathrm{NP}}\Psi_I(\mathbf{x})=1\\ \sum_{I=1}^{\mathrm{NP}}[\Psi_I^1(\mathbf{x})+\Psi_I^2(\mathbf{x})]x_I&=\sum_{I=1}^{\mathrm{NP}}\Psi_I(\mathbf{x})x_I=x\\ \sum_{I=1}^{\mathrm{NP}}[\Psi_I^1(\mathbf{x})+\Psi_I^2(\mathbf{x})]y_I&=\sum_{I=1}^{\mathrm{NP}}\Psi_I(\mathbf{x})y_I=y\\ \sum_{I=1}^{\mathrm{NP}}[\Psi_I^1(\mathbf{x})+\Psi_I^2(\mathbf{x})]z_I&=\sum_{I=1}^{\mathrm{NP}}\Psi_I(\mathbf{x})z_I=z\end{aligned} \tag{17}$$

Thus the approximation of u by this constrained RK using NP physical nodes is

$$u^h(\mathbf{x})=\sum_{I=1}^{\mathrm{NP}}\Psi_I(\mathbf{x})u_I \tag{18}$$

where

$$\Psi_I(\mathbf{x}) = \Psi_I^1(\mathbf{x}) + \Psi_I^2(\mathbf{x}), \quad 1 \leqslant I \leqslant \mathrm{NP} \tag{19}$$

3.2. Pseudo-inverse method

We first analyse the cause of singularity in the moment matrix $\mathbf{M}$ in Equation (5). Note that $\mathbf{M}$ is the Gram matrix associated with basis functions $\mathbf{H}^{\mathrm{T}}(\mathbf{x}-\mathbf{x}_I) = [1 \;\; x - x_I \;\; y_2 - y_I \;\; z - z_I \;\; (x-x_I)^2 \;\; \cdots \;\; (z-z_I)^n]$ with respect to kernel $\phi_a(\mathbf{x}-\mathbf{x}_I)$. If shell surface function is expressible by the linear combination of basis functions as $F(\mathbf{x}) = \sum_{i+j+k=0}^{n} a_{ijk} h_{ijk} (\mathbf{x}-\mathbf{x}_I) = 0$, where $h_{ijk}(\mathbf{x}-\mathbf{x}_I) = (x-x_I)^i (y-y_I)^j (z-z_I)^k$, the surface function $F(\mathbf{x}) = 0$ introduces a linear dependency in the basis functions. This leads to a singularity in the moment matrix $\mathbf{M}$. Let the shell surface function be expressed as

$$F(\mathbf{x}) = \mathbf{H}^{\mathrm{T}}(\mathbf{x}-\mathbf{x}_I)\mathbf{a} = 0 \tag{20}$$

Since discrete points $\mathbf{x}_I$ are on the shell surface, setting $\mathbf{x} = \mathbf{x}_I$ leads to the following condition for the coefficients:

$$a_{000} = 0 \tag{21}$$

Using Equation (20), we have

$$\mathbf{Ma} = \left(\sum_{I=1}^{\mathrm{NP}} \mathbf{H}\mathbf{H}^{\mathrm{T}} \phi_a \right) \mathbf{a} = \sum_{I=1}^{\mathrm{NP}} \mathbf{H}(\mathbf{H}^{\mathrm{T}}\mathbf{a})\phi_a = \mathbf{0} \tag{22}$$

Combination of Equations (21) and (22) indicates that the coefficients in the linear combination of surface function in Equation (20), $\mathbf{a}^{\mathrm{T}} = [0, a_{100}, \ldots, a_{00n}]$, span the null space of $\mathbf{M}$ with nullity of 1. Note that $\mathbf{a}^{\mathrm{T}} = [0, a_{100}, \ldots, a_{00n}]$ is orthogonal to $\mathbf{H}(\mathbf{0})$, and hence $\mathbf{H}(\mathbf{0})$ is orthogonal to the null space of $\mathbf{M}$. Thus Equation (5) can be solved with a pseudo-inverse approach.

The eigenvector expansion of $\mathbf{M}$ is expressed as

$$\mathbf{M} = \sum_{i=1}^{m} p_i \mathbf{v}_i \otimes \mathbf{v}_i \tag{23}$$

where m is the total number of nonzero eigenvalues, and p_i's, and $\mathbf{v}_i$'s are the eigenvalues and eigenvectors of $\mathbf{M}$, respectively. Since $\mathbf{H}(\mathbf{0})$ is orthogonal to the null space of moment matrix $\mathbf{M}$, Equation (5) can be solved as

$$\mathbf{b}(\mathbf{x}) = \tilde{\mathbf{M}}^{-1}\mathbf{H}(\mathbf{0}) \tag{24}$$

where

$$\tilde{\mathbf{M}}^{-1} = \sum_{i=1}^{m} p_i^{-1} \mathbf{v}_i \otimes \mathbf{v}_i \tag{25}$$

With this pseudo-inverse approach, the coefficients $\mathbf{b}(\mathbf{x})$ and consequently the RK shape function $\Psi_I(\mathbf{x})$ can be directly obtained from Equations (5) and (3). In the case where the moment matrix is nonsingular, this pseudo-inverse recovers the standard definition of matrix inverse.

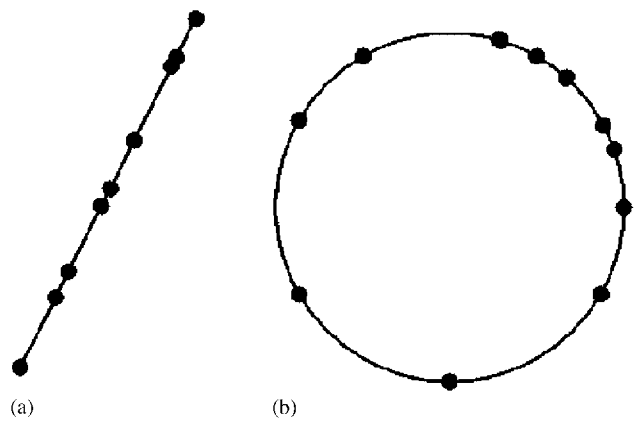

Figure 2. Representation of constrained geometry.

Table I. Line representation using the constrained RK approximation. (a) Dummy node method, (b) pseudo-inverse method.

Node	x_I	y_I	$\sum \Psi_I$	$\sum \Psi_I x_I$	$\sum \Psi_I y_I$
(*a*)					
1	0.05000	0.10000	1.00032	0.05030	0.10060
2	0.85000	1.70000	1.00016	0.85013	1.70026
3	1.15000	2.30000	0.99998	1.14997	2.29993
4	1.90000	3.80000	1.00012	1.90020	3.80039
5	2.10000	4.20000	0.99998	2.09997	4.19993
6	2.65000	5.30000	0.99976	2.64934	5.29868
7	3.50000	7.00000	1.00018	3.50059	7.00117
8	3.60000	7.20000	1.00007	3.60023	7.20046
9	4.05000	8.10000	0.99950	4.04824	8.09648
(*b*)					
1	0.05000	0.10000	1.00000	0.05000	0.10000
2	0.85000	1.70000	1.00000	0.85000	1.70000
3	1.15000	2.30000	1.00000	1.15000	2.30000
4	1.90000	3.80000	1.00000	1.90000	3.80000
5	2.10000	4.20000	1.00000	2.10000	4.20000
6	2.65000	5.30000	1.00000	2.65000	5.30000
7	3.50000	7.00000	1.00000	3.50000	7.00000
8	3.60000	7.20000	1.00000	3.60000	7.20000
9	4.05000	8.10000	1.00000	4.05000	8.10000

3.3. Examples

Two geometries, a straight line and a circle as shown in Figure 2, are considered to illustrate how the proposed methods overcome the singularity in the Cartesian kernel reproducing functions.

3.3.1. Straight line representation. The nodal coordinates of a straight line with randomly distributed nodes are shown in Figure 2(a) and listed in Table I. Employing the conventional

Table II. Circular ring representation using a constrained RK approximation on a set of co-circular nodes. (a) Dummy node method, (b) pseudo-inverse method.

Node	x_I	y_I	x_I^2	y_I^2	$\sum \Psi_I$	$\sum \Psi_I x_I$	$\sum \Psi_I y_I$	$\sum \Psi_I x_I^2$	$\sum \Psi_I y_I^2$
(*a*)									
1	10.00000	0.00000	100.00000	0.00000	1.00003	10.00013	0.00021	99.99932	0.00345
2	6.69131	7.43145	44.77358	55.22642	1.00001	6.69137	7.43151	44.77442	55.22708
3	5.00000	8.66025	25.00000	75.00000	1.00001	5.00011	8.66029	25.00187	74.99946
4	8.82948	4.69472	77.95965	22.04035	1.00002	8.82954	4.69484	77.95881	22.04304
5	−5.00000	8.66025	25.00000	75.00000	1.00003	−4.99990	8.66048	25.00192	75.00145
6	−8.66025	5.00000	75.00000	25.00000	1.00002	−8.66026	5.00014	74.99896	25.00341
7	2.92372	9.56305	8.54812	91.45188	1.00002	2.92385	9.56310	8.55145	91.45056
8	−8.66025	−5.00000	75.00000	25.00000	1.00002	−8.66032	−5.00000	75.00013	25.00214
9	2.80427	9.59875	7.86395	92.13605	1.00002	2.80441	9.59881	7.86735	92.13470
10	−0.00000	−10.00000	0.00000	100.00000	1.00003	0.00003	−10.00006	0.00351	99.99909
11	9.43057	3.32631	88.93563	11.06437	1.00002	9.43064	3.32647	88.93447	11.06768
12	8.66025	−5.00000	75.00000	25.00000	1.00003	8.66050	−4.99982	75.00266	25.00074
(*b*)									
1	10.00000	0.00000	100.00000	0.00000	1.00000	10.00000	0.00000	100.00000	0.00000
2	6.69131	7.43145	44.77358	55.22642	1.00000	6.69131	7.43145	44.77358	55.22642
3	5.00000	8.66025	25.00000	75.00000	1.00000	5.00000	8.66025	25.00000	75.00000
4	8.82948	4.69472	77.95965	22.04035	1.00000	8.82948	4.69472	77.95965	22.04035
5	−5.00000	8.66025	25.00000	75.00000	1.00000	−5.00000	8.66025	25.00000	75.00000
6	−8.66025	5.00000	75.00000	25.00000	1.00000	−8.66025	5.00000	75.00000	25.00000
7	2.92372	9.56305	8.54812	91.45188	1.00000	2.92372	9.56305	8.54812	91.45188
8	−8.66025	−5.00000	75.00000	25.00000	1.00000	−8.66025	−5.00000	75.00000	25.00000
9	2.80427	9.59875	7.86395	92.13605	1.00000	2.80427	9.59875	7.86395	92.13605
10	0.00000	−10.00000	0.00000	100.00000	1.00000	0.00000	−10.00000	0.00000	100.00000
11	9.43057	3.32631	88.93563	11.06437	1.00000	9.43057	3.32631	88.93563	11.06437
12	8.66025	−5.00000	75.00000	25.00000	1.00000	8.66025	−5.00000	75.00000	25.00000

RK approximation in two dimensions leads to a singular moment matrix **M** when linear reproducing conditions are imposed in Cartesian coordinates. In this particular case, since $(y - y_I) = c(x - x_I)$, it can be easily seen that the rows (and columns) in the **M** matrix are proportional to each other and thus leads to singularity. The reproduction of constant and linear functions using the constrained RK approximation using both dummy node method with $t_1 = t_2 = 0.001$ and the pseudo-inverse method are shown in Table I. The results in Table I shows that the dummy node approximation leads to an error $\propto t$, whereas pseudo-inverse approach exactly reproduces linear function. On the other hand, pseudo-inverse approach requires solving an eigenvalue problem, whereas the effort in constructing constrained RK approximation using dummy node is very similar to that of the standard RK approximation.

3.3.2. Representation of a circular ring. In a parametric-based CAD representation of a circular ring, at least four parametric domains are required. It is not possible to construct reproducing kernel shape functions with nodes located in four parametric systems. On the other hand, using Cartesian coordinates with quadratic basis functions in the RK approximation on a ring results in a singular moment matrix **M**, since the second-order reproducing equations are linearly dependent to the ring function. The results in Table II show that this singularity in **M** can be resolved by the proposed constrained RK shape functions even when a second-order basis in Cartesian coordinate is used. The reproduction of zeroth-, first-, and second-order functions by the constrained RK shape functions using both dummy node method with $t_1 = t_2 = 0.001$ and the pseudo-inverse method are compared in Table II. The results again shows that the constrained RK approximation leads to an error $\propto t$, whereas pseudo-inverse approach exactly reproduces linear and quadratic functions.

4. CONSTRAINED RK SHEAR DEFORMABLE SHELL FORMULATION IN CARTESIAN COORDINATES

Let the shell surface be discretized by a set of points in a fixed global Cartesian coordinate. At a shell mid-surface location $\mathbf{x}$, a local coordinate system with basis vectors $\hat{\mathbf{e}}_1, \hat{\mathbf{e}}_2, \hat{\mathbf{e}}_3$ is defined, where $\hat{\mathbf{e}}_1$ and $\hat{\mathbf{e}}_2$ are tangent unit vectors, and $\hat{\mathbf{e}}_3$ is a unit vector normal to the surface as shown in Figure 3.

The displacement vector $\mathbf{u}(\mathbf{x})$ in a shell structure is represented by the combination of translational and rotational degrees of freedom as

$$\mathbf{u}(\mathbf{x}) = \underbrace{\mathbf{u}^{\mathrm{t}}(\mathbf{x})}_{\text{Translation}} + \underbrace{\mathbf{u}^{\mathrm{r}}(\mathbf{x})}_{\text{Rotation}} \tag{26}$$

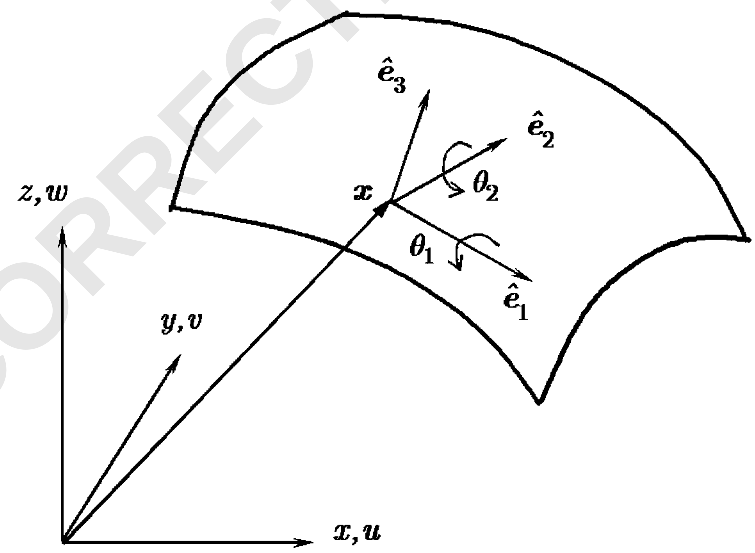

Figure 3. Sign conventions in shell formulation.

Using the local coordinates, this displacement vector can be expressed as

$$\hat{\mathbf{u}}(\mathbf{x}) = \begin{pmatrix} \hat{u} \\ \hat{v} \\ \hat{w} \end{pmatrix} = \begin{pmatrix} \hat{u}^{\mathrm{t}} \\ \hat{v}^{\mathrm{t}} \\ \hat{w}^{\mathrm{t}} \end{pmatrix} + \begin{pmatrix} \hat{z}\theta_2 \\ -\hat{z}\theta_1 \\ 0 \end{pmatrix} \tag{27}$$

where $\hat{z}$ is the local coordinate in the $\hat{\mathbf{e}}_3$ direction, and the sign convention of the cross sectional rotations θ_1 and θ_2 is shown in Figure 3. Following Equation (27), the strain components in the local coordinate system are expressed as

$$\hat{\boldsymbol{\varepsilon}} = \begin{pmatrix} \hat{\varepsilon}_{11} \\ \hat{\varepsilon}_{22} \\ \hat{\gamma}_{12} \\ \hat{\gamma}_{23} \\ \hat{\gamma}_{13} \end{pmatrix} = \begin{pmatrix} \dfrac{\partial \hat{u}}{\partial \hat{x}} \\ \dfrac{\partial \hat{v}}{\partial \hat{y}} \\ \dfrac{\partial \hat{u}}{\partial \hat{y}} + \dfrac{\partial \hat{v}}{\partial \hat{x}} \\ \dfrac{\partial \hat{u}}{\partial \hat{z}} + \dfrac{\partial \hat{w}}{\partial \hat{x}} \\ \dfrac{\partial \hat{v}}{\partial \hat{z}} + \dfrac{\partial \hat{w}}{\partial \hat{y}} \end{pmatrix} \tag{28}$$

The strain $\hat{\boldsymbol{\varepsilon}}$ can be split into membrane strain $\hat{\boldsymbol{\varepsilon}}^{\mathrm{m}}$ shear strain $\hat{\boldsymbol{\varepsilon}}^{\mathrm{s}}$, and bending strain $\hat{\boldsymbol{\varepsilon}}^{\mathrm{b}}$ as follows:

$$\hat{\boldsymbol{\varepsilon}} = \begin{pmatrix} \hat{\boldsymbol{\varepsilon}}^{\mathrm{m}} + \hat{\boldsymbol{\varepsilon}}^{\mathrm{b}} \\ \hat{\boldsymbol{\varepsilon}}^{\mathrm{s}} \end{pmatrix} \tag{29}$$

where

$$\hat{\boldsymbol{\varepsilon}}^{\mathrm{m}} = \begin{pmatrix} \dfrac{\partial \hat{u}^{\mathrm{t}}}{\partial \hat{x}} \\ \dfrac{\partial \hat{v}^{\mathrm{t}}}{\partial \hat{y}} \\ \dfrac{\partial \hat{u}^{\mathrm{t}}}{\partial \hat{y}} + \dfrac{\partial \hat{v}^{\mathrm{t}}}{\partial \hat{x}} \end{pmatrix}, \quad \hat{\boldsymbol{\varepsilon}}^{\mathrm{b}} = \hat{z}\boldsymbol{\kappa} = \hat{z} \begin{pmatrix} \dfrac{\partial \theta_2}{\partial \hat{x}} \\ -\dfrac{\partial \theta_1}{\partial \hat{y}} \\ \dfrac{\partial \theta_2}{\partial \hat{y}} - \dfrac{\partial \theta_1}{\partial \hat{x}} \end{pmatrix}, \quad \hat{\boldsymbol{\varepsilon}}^{\mathrm{s}} = \begin{pmatrix} \dfrac{\partial \hat{w}^{\mathrm{t}}}{\partial \hat{x}} + \theta_2 \\ \dfrac{\partial \hat{w}^{\mathrm{t}}}{\partial \hat{y}} - \theta_1 \end{pmatrix} \tag{30}$$

with $\boldsymbol{\kappa}$ denoting the curvature.

In a shear deformable shell formulation, the variational equation can be expressed as

$$\int_{\Omega} \delta \hat{\boldsymbol{\varepsilon}}^{\mathrm{T}} \hat{\mathbf{C}} \hat{\boldsymbol{\varepsilon}} \, \mathrm{d}\Omega - \delta W^{\mathrm{ext}} = 0 \tag{31}$$

where $\hat{\mathbf{C}}$ is the elasticity matrix in the local coordinate system. For linear isotropic material, the stress–strain law is

$$\hat{\boldsymbol{\sigma}} = \hat{\mathbf{C}}\hat{\boldsymbol{\varepsilon}} \tag{32}$$

where

$$\hat{\boldsymbol{\sigma}} = [\hat{\sigma}_{11} \quad \hat{\sigma}_{22} \quad \hat{\sigma}_{12} \quad \hat{\sigma}_{23} \quad \hat{\sigma}_{13}]^{\mathrm{T}}, \quad \hat{\sigma}_{33} = 0 \tag{33}$$

$$\hat{\mathbf{C}} = \frac{E}{1-v^2}\begin{pmatrix} 1 & v & 0 & 0 & 0 \\ v & 1 & 0 & 0 & 0 \\ 0 & 0 & \dfrac{1-v}{2} & 0 & 0 \\ 0 & 0 & 0 & k\dfrac{(1-v)}{2} & 0 \\ 0 & 0 & 0 & 0 & k\dfrac{(1-v)}{2} \end{pmatrix}, \quad k = \frac{5}{6} \tag{34}$$

Let the global displacement vector be approximated by Cartesian constrained RK shape functions as

$$\begin{pmatrix} u \\ v \\ w \end{pmatrix} = \sum_I \Psi_I(\mathbf{x}) \begin{pmatrix} u_I \\ v_I \\ w_I \end{pmatrix} + \sum_I \frac{t\zeta}{2}\Psi_I(\mathbf{x})[\hat{\mathbf{e}}_{I1} \quad -\hat{\mathbf{e}}_{I2}]\begin{pmatrix} \theta_{I2} \\ \theta_{I1} \end{pmatrix} \tag{35}$$

where ζ is the thickness variable, and $\hat{z} = \zeta t/2$.

The local displacement vector, $\hat{\mathbf{u}}$, can be related to the global displacement $\mathbf{u}$ vector by a coordinate transformation:

$$\begin{pmatrix} \hat{u} \\ \hat{v} \\ \hat{w} \end{pmatrix} = \mathbf{Qu} = \sum_I \Psi_I(\mathbf{x})[\mathbf{Q} \quad \hat{z}\overline{\mathbf{Q}}]\mathbf{d}_I \tag{36}$$

where $\mathbf{Q}$, $\overline{\mathbf{Q}}$ and $\mathbf{d}_I$ are defined as

$$\mathbf{Q}(\mathbf{x}) = \begin{pmatrix} \hat{\mathbf{e}}_1^{\mathrm{T}}(\mathbf{x}) \\ \hat{\mathbf{e}}_2^{\mathrm{T}}(\mathbf{x}) \\ \hat{\mathbf{e}}_3^{\mathrm{T}}(\mathbf{x}) \end{pmatrix} = \begin{pmatrix} l_1 & m_1 & n_1 \\ l_2 & m_2 & n_2 \\ l_3 & m_3 & n_3 \end{pmatrix} \tag{37}$$

$$\overline{\mathbf{Q}} = \mathbf{Q}[\hat{\mathbf{e}}_{I1} \quad -\hat{\mathbf{e}}_{I2}] = \begin{pmatrix} \hat{\mathbf{e}}_1^{\mathrm{T}}\hat{\mathbf{e}}_{I1} & -\hat{\mathbf{e}}_1^{\mathrm{T}}\hat{\mathbf{e}}_{I2} \\ \hat{\mathbf{e}}_2^{\mathrm{T}}\hat{\mathbf{e}}_{I1} & -\hat{\mathbf{e}}_2^{\mathrm{T}}\hat{\mathbf{e}}_{I2} \\ \hat{\mathbf{e}}_3^{\mathrm{T}}\hat{\mathbf{e}}_{I1} & -\hat{\mathbf{e}}_3^{\mathrm{T}}\hat{\mathbf{e}}_{I2} \end{pmatrix} \tag{38}$$

$$\mathbf{d}_I = [u_I \quad v_I \quad w_I \quad \theta_{I2} \quad \theta_{I1}]^{\mathrm{T}} \tag{39}$$

and (l_i, m_i, n_i) are direction cosines between local axis $\hat{\mathbf{e}}_i$ and global axes.

By means of the strain–displacement relation of Equation (28), the local strain can be expressed as

$$\hat{\boldsymbol{\varepsilon}}(\mathbf{x}_L) = \underbrace{\sum_I \mathbf{B}_I^{\mathrm{m-s}}(\mathbf{x}_L)\mathbf{d}_I}_{\hat{\boldsymbol{\varepsilon}}^{\mathrm{m}}+\hat{\boldsymbol{\varepsilon}}^{\mathrm{s}}} + \underbrace{\sum_I \hat{z}\mathbf{B}_I^{\mathrm{b}}(\mathbf{x}_L)\mathbf{d}_I}_{\hat{\boldsymbol{\varepsilon}}^{\mathrm{b}}} \tag{40}$$

where

$$\mathbf{B}_I^{\mathrm{m-s}} = \begin{pmatrix} \frac{\partial \Psi_I}{\partial \hat{x}} l_1 & \frac{\partial \Psi_I}{\partial \hat{x}} m_1 & \frac{\partial \Psi_I}{\partial \hat{x}} n_1 & 0 & 0 \\ \frac{\partial \Psi_I}{\partial \hat{y}} l_2 & \frac{\partial \Psi_I}{\partial \hat{y}} m_2 & \frac{\partial \Psi_I}{\partial \hat{y}} n_2 & 0 & 0 \\ \frac{\partial \Psi_I}{\partial \hat{y}} l_1 + \frac{\partial \Psi_I}{\partial \hat{x}} l_2 & \frac{\partial \Psi_I}{\partial \hat{y}} m_1 + \frac{\partial \Psi_I}{\partial \hat{x}} m_2 & \frac{\partial \Psi_I}{\partial \hat{y}} n_1 + \frac{\partial \Psi_I}{\partial \hat{x}} n_2 & 0 & 0 \\ \frac{\partial \Psi_I}{\partial \hat{y}} l_3 & \frac{\partial \Psi_I}{\partial \hat{y}} m_3 & \frac{\partial \Psi_I}{\partial \hat{y}} n_3 & \Psi_I \overline{Q}_{21} & \Psi_I \overline{Q}_{22} \\ \frac{\partial \Psi_I}{\partial \hat{x}} l_3 & \frac{\partial \Psi_I}{\partial \hat{x}} m_3 & \frac{\partial \Psi_I}{\partial \hat{x}} n_3 & \Psi_I \overline{Q}_{11} & \Psi_I \overline{Q}_{12} \end{pmatrix} \tag{41}$$

$$\mathbf{B}_I^{\mathrm{b}} = \begin{pmatrix} 0 & 0 & 0 & \frac{\partial \Psi_I}{\partial \hat{x}} \overline{Q}_{11} & \frac{\partial \Psi_I}{\partial \hat{x}} \overline{Q}_{12} \\ 0 & 0 & 0 & \frac{\partial \Psi_I}{\partial \hat{y}} \overline{Q}_{21} & \frac{\partial \Psi_I}{\partial \hat{y}} \overline{Q}_{22} \\ 0 & 0 & 0 & \frac{\partial \Psi_I}{\partial \hat{y}} \overline{Q}_{11} + \frac{\partial \Psi_I}{\partial \hat{x}} \overline{Q}_{21} & \frac{\partial \Psi_I}{\partial \hat{y}} \overline{Q}_{12} + \frac{\partial \Psi_I}{\partial \hat{x}} \overline{Q}_{22} \\ 0 & 0 & 0 & \frac{\partial \Psi_I}{\partial \hat{y}} \overline{Q}_{31} & \frac{\partial \Psi_I}{\partial \hat{y}} \overline{Q}_{32} \\ 0 & 0 & 0 & \frac{\partial \Psi_I}{\partial \hat{x}} \overline{Q}_{31} & \frac{\partial \Psi_I}{\partial \hat{x}} \overline{Q}_{32} \end{pmatrix} \tag{42}$$

The derivative of constrained RK shape function with respect to the local coordinates is computed as

$$\frac{\partial \Psi_I}{\partial \hat{x}_j} = \frac{\partial \Psi_I}{\partial x_k}\frac{\partial x_k}{\partial \hat{x}_j} = Q_{jk}\frac{\partial \Psi_I}{\partial x_k} = l_j\frac{\partial \Psi_I}{\partial x} + m_j\frac{\partial \Psi_I}{\partial y} + n_j\frac{\partial \Psi_I}{\partial z} \tag{43}$$

The resulting stiffness matrix is then obtained by

$$\begin{aligned}\mathbf{K} &= \int_\Omega (\mathbf{B}^{\mathrm{m-s}^{\mathrm{T}}} + \hat{z}\mathbf{B}^{\mathrm{b}^{\mathrm{T}}})\hat{\mathbf{C}}(\mathbf{B}^{\mathrm{m-s}} + \hat{z}\mathbf{B}^{\mathrm{b}})\,\mathrm{d}\Omega \\ &= t\int_A \mathbf{B}^{\mathrm{m-s}^{\mathrm{T}}}\hat{\mathbf{C}}\mathbf{B}^{\mathrm{m-s}}\,\mathrm{d}A + \frac{t^3}{12}\int_A \mathbf{B}^{\mathrm{b}^{\mathrm{T}}}\hat{\mathbf{C}}\mathbf{B}^{\mathrm{b}}\,\mathrm{d}A \\ &= \mathbf{K}^{\mathrm{m-s}} + \mathbf{K}^{\mathrm{b}}\end{aligned} \tag{44}$$

5. STABILIZATION OF NODAL INTEGRATION IN SHELL DOMAIN INTEGRATION

A critical issue to be addressed in the shear deformable shell formulation is the removal of shear and membrane locking in the limit of thin shell. In this study, this is achieved by introducing a nodal integration with stabilization in the domain integration of the discrete equations. To avoid locking and maintain stability [10], the membrane and shear energies are integrated by a direct nodal integration, whereas nodal integration with stabilization is introduced for the bending energy.

To stabilize nodal integration for bending strain energy, a curvature smoothing is considered. Although the curvature smoothing is to be performed on the shell curved mid-surface, it is more convenient to consider the shell curved mid-surface as a limiting geometry of a 3D solid representation of shell structure when thickness approaches zero. Here, a nodal representative volume Ω_L of node L with thickness t and mid-surface area A_L for node $\mathbf{x}_L$ as shown in Figure 4(a) is defined. As shown in Figure 4(b), the upper and lower surfaces of this volume

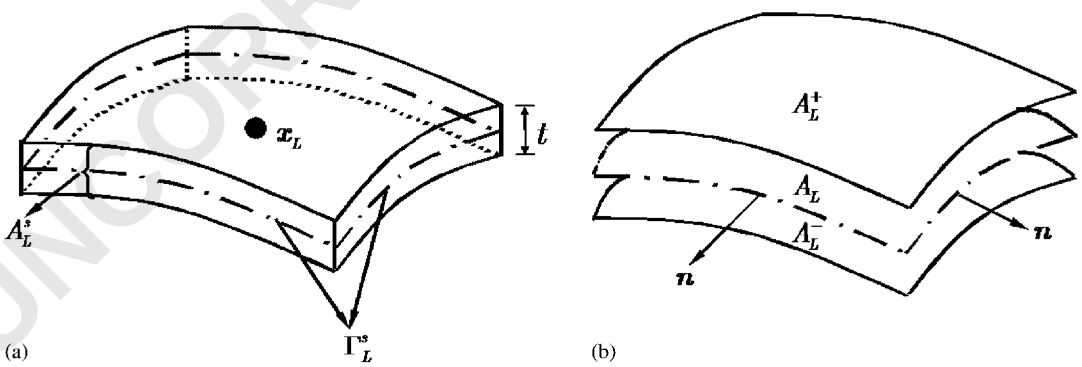

Figure 4. Solid representation of nodal domain for a node on shell surface.

are denoted as A_L^+ and A_L^-, respectively, and they approach A_L as $t \to 0$. The boundary S_L of Ω_L can be expressed by

$$S_L = A_L^+ \cup A_L^- \cup A_L^{\mathrm{s}} \tag{45}$$

where A_L^{s} is the through-thickness area of the nodal representative volume as shown in Figure 4(a).

We first define the smoothed gradient of shape function at the node L over the nodal representative domain Ω_L following References [11–13] as

$$\tilde{\nabla}_i \Psi_I(\mathbf{x}_L) = \frac{1}{V_L} \int_{\Omega_L} \Psi_{I,i}(\mathbf{x})\, \mathrm{d}\Omega = \frac{1}{A_L t} \int_{S_L} \Psi_I(\mathbf{x}) n_i \, \mathrm{d}S \tag{46}$$

where $V_L = \int_{\Omega_L} \mathrm{d}\Omega$ and $\mathbf{n}$ is the surface normal. Using Equation (45), the integral in Equation (46) can be expressed as a summation of three surface integrals:

$$\int_{S_L} \Psi_I(\mathbf{x}) n_i \, \mathrm{d}S = \int_{A_L^+} \Psi_I(\mathbf{x}) n_i \, \mathrm{d}S + \int_{A_L^-} \Psi_I(\mathbf{x}) n_i \, \mathrm{d}S + \int_{A_L^{\mathrm{s}}} \Psi_I(\mathbf{x}) n_i \, \mathrm{d}S \tag{47}$$

As $t \to 0$, $\int_{A_L^+} \Psi_I(\mathbf{x}) n_i \, \mathrm{d}S \to -\int_{A_L^-} \Psi_I(\mathbf{x}) n_i \, \mathrm{d}S$, and Equation (47) reduces to

$$\int_{S_L} \Psi_I(\mathbf{x}) n_i \, \mathrm{d}S = \int_{A_L^{\mathrm{s}}} \Psi_I(\mathbf{x}) n_i \, \mathrm{d}S \tag{48}$$

Since $\Psi_I(\mathbf{x})$ and n_i are defined on the shell mid-surface and not functions of t, Equation (48) further reduces to

$$\int_{A_L^{\mathrm{s}}} \Psi_I(\mathbf{x}) n_i \, \mathrm{d}S = t \int_{\Gamma_L^{\mathrm{s}}} \Psi_I(\mathbf{x}) n_i \, \mathrm{d}\Gamma \tag{49}$$

where Γ_L^{s} is the contour surrounding the mid-surface of the nodal representative domain V_L, and $\mathbf{n}$ is the surface tangent of the shell mid-surface along and normal to the contour Γ_L^{s}. Finally, the smoothed gradient of shape function can be expressed as

$$\tilde{\nabla}_i \Psi_I(\mathbf{x}_L) = \frac{1}{V_L} \int_{S_L} \Psi_I(\mathbf{x}) n_i \, \mathrm{d}S = \frac{1}{A_L} \int_{\Gamma_L^{\mathrm{s}}} \Psi_I(\mathbf{x}) n_i \, \mathrm{d}\Gamma \tag{50}$$

With this smoothing of shape function gradient in the global coordinates, the smoothing of the shape function gradients in the local gradient can be obtained using Equation (43):

$$\tilde{\nabla}_{\hat{j}} \Psi_I = l_j \tilde{\nabla}_x \Psi_I + m_j \tilde{\nabla}_y \Psi_I + n_j \tilde{\nabla}_z \Psi_I \tag{51}$$

This smoothed gradient is introduced to the curvature to yield

$$\tilde{\boldsymbol{\kappa}}(\mathbf{x}_L) = \frac{1}{A_L} \int_{A_L} \boldsymbol{\kappa} \, \mathrm{d}A = \frac{1}{A_L} \int_{\Gamma_L^{\mathrm{s}}} \begin{pmatrix} \theta_2 n_1 \\ -\theta_1 n_2 \\ -\theta_1 n_1 + \theta_2 n_2 \end{pmatrix} \mathrm{d}\Gamma \tag{52}$$

Introducing RK approximation equation (35) into Equation (52) gives

$$\tilde{\boldsymbol{\kappa}}(\mathbf{x}_L) = \sum_{I=1}^{\mathrm{NP}} \tilde{\mathbf{B}}_I^{\mathrm{b}}(\mathbf{x}_L)\mathbf{d}_I \tag{53}$$

Further considering that at the nodal point we have

$$\overline{\mathbf{Q}}(\mathbf{x}_I) = \mathbf{Q}(\mathbf{x}_I)[\hat{\mathbf{e}}_{I1} \quad -\hat{\mathbf{e}}_{I2}] = \begin{pmatrix} 1 & 0 \\ 0 & -1 \\ 0 & 0 \end{pmatrix} \tag{54}$$

Thus the smoothed bending gradient matrix becomes

$$\tilde{\mathbf{B}}_I^{\mathrm{b}} = \begin{pmatrix} 0 & 0 & 0 & \tilde{\nabla}_{\hat{x}}\Psi_I & 0 \\ 0 & 0 & 0 & 0 & -\tilde{\nabla}_{\hat{y}}\Psi_I \\ 0 & 0 & 0 & \tilde{\nabla}_{\hat{y}}\Psi_I & -\tilde{\nabla}_{\hat{x}}\Psi_I \\ 0 & 0 & 0 & 0 & 0 \\ 0 & 0 & 0 & 0 & 0 \end{pmatrix} \tag{55}$$

Employing stabilized nodal integration for bending stiffness and direct nodal integration for membrane–shear stiffness, the stiffness takes the form

$$\mathbf{K}_{IJ} = \sum_{L=1}^{\mathrm{NP}} A_L \left[t\tilde{\mathbf{B}}_I^{\mathrm{b}^{\mathrm{T}}}(\mathbf{x}_L)\hat{\mathbf{C}}\tilde{\mathbf{B}}_J^{\mathrm{b}}(\mathbf{x}_L) + \frac{t^3}{12}\mathbf{B}_I^{\mathrm{m-s}^{\mathrm{T}}}(\mathbf{x}_L)\hat{\mathbf{C}}\mathbf{B}_J^{\mathrm{m-s}}(\mathbf{x}_L) \right] \tag{56}$$

6. NUMERICAL EXAMPLES

In the following examples, the quadratic basis and a normalized support size of 3.0 are employed in the constrained RK approximation.

6.1. Scordelis-Lo roof

The Scodelis-Lo roof subjected to a self-weight $q = 90$ per unit area is depicted in Figure 5. This is a classical problem to evaluate the ability of a numerical method to model membrane behaviour. The geometric parameters are: roof length $L = 50$, radius $R = 25$, thickness $t = 0.25$, and the vertex angle of the arc $\theta = 80°$. The material properties are Young's modulus $E = 4.32 \times 10^8$ and Poisson ratio $v = 0$. According to Reference [14], a reference solution for the deflection at the centre of the free edge (A) is 0.3024. Due to symmetry of the structure, only a quarter of the roof is modelled. Normalized values of the transverse displacement at point A obtained using different discretizations are plotted in Figure 6. FEM solutions using nine-node element with selective reduced integration (SRI) [15] and other elements (RSDS, References [15, 16]) are also plotted for comparison purposes. The numerical results show good solution of the proposed method compared with several published finite element solutions.

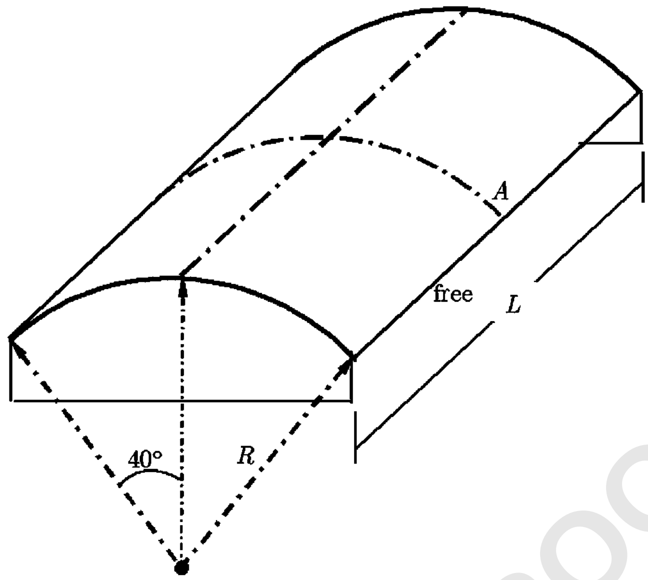

Figure 5. Geometry of Scordelis-Lo roof.

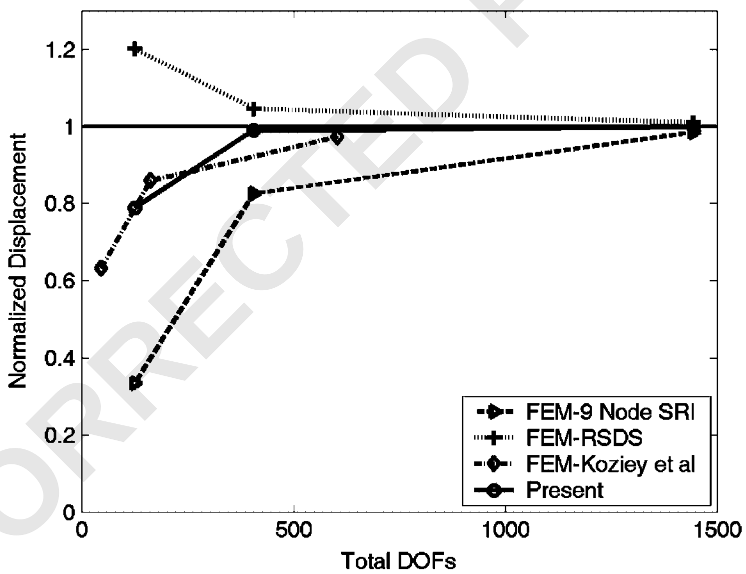

Figure 6. Comparison of normalized displacements underneath point load in the Scordelis-Lo roof.

6.2. Hemispherical shell with 18° *hole*

A hemispherical shell with radius $R = 10.0$ and thickness $t = 0.04$, subjected to two equal and opposite forces in the global x and y directions as shown in Figure 7 is analysed.

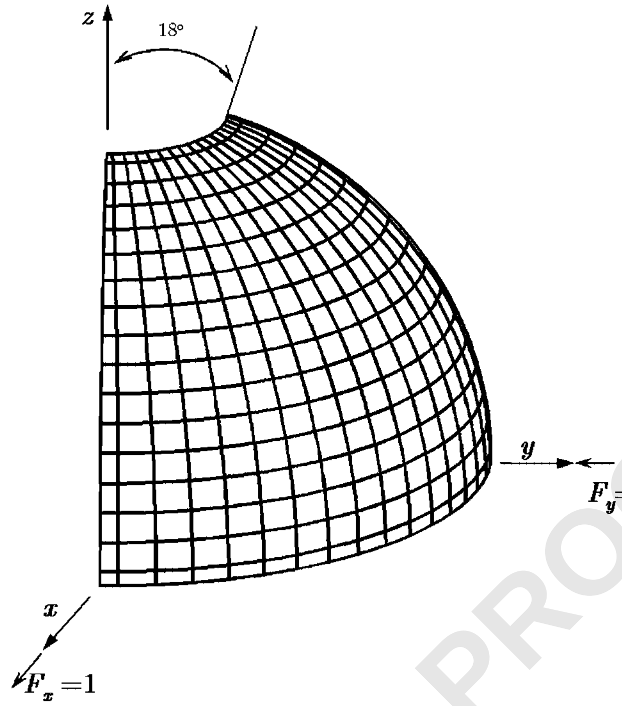

Figure 7. Geometry of hemispherical shell.

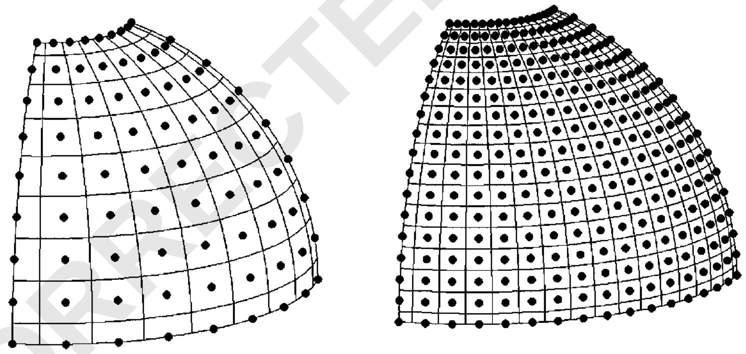

Figure 8. Meshfree discretizations of hemispherical shell.

The material constants are: Young's modulus $E = 6.825 \times 10^7$ and Poisson ratio $\nu = 0.3$. The reference solution of deflection under the point load is 0.093 [15]. Various discretizations as shown in Figure 8 are employed in the analysis. The normalized transverse deflections under point load obtained by the proposed method are compared with the FEM solutions obtained using nine-node element with SRI [17], nine-node shell element QUAD9** [18], and discrete Kirchhoff quadrilateral element DKQ [19] as shown in Figure 9. Note that since DKQ method excludes shear energy, and it is only applicable to thin shell structures. The numerical results

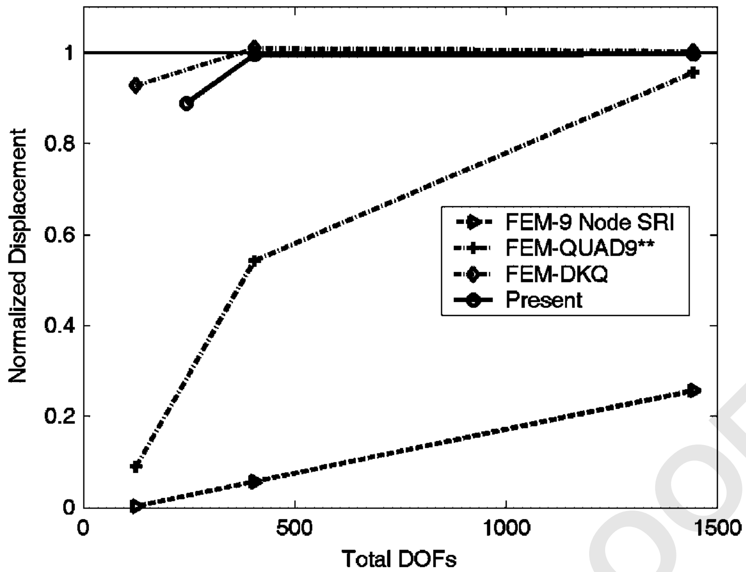

Figure 9. Comparison of normalized displacements underneath point load in the hemispherical shell.

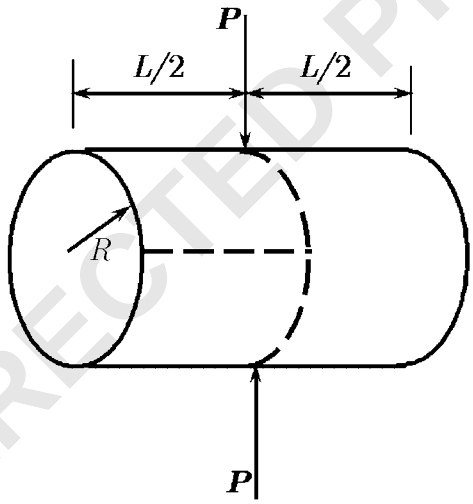

Figure 10. Problem statement of pinched cylinder with free ends.

show that the present approach performs very well compared to other well-known finite element solutions.

6.3. *Pinched cylinder with free ends*

The problem statement of this problem is shown in Figure 10, where the length, radius and thickness are selected as $L = 10.35$, $R = 5.0$, and $t = 0.094$. The material constants are Young's

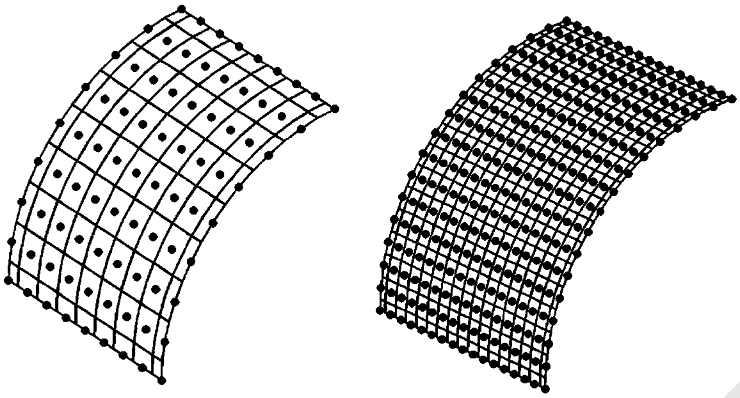

Figure 11. Meshfree discretization of pinched cylinder.

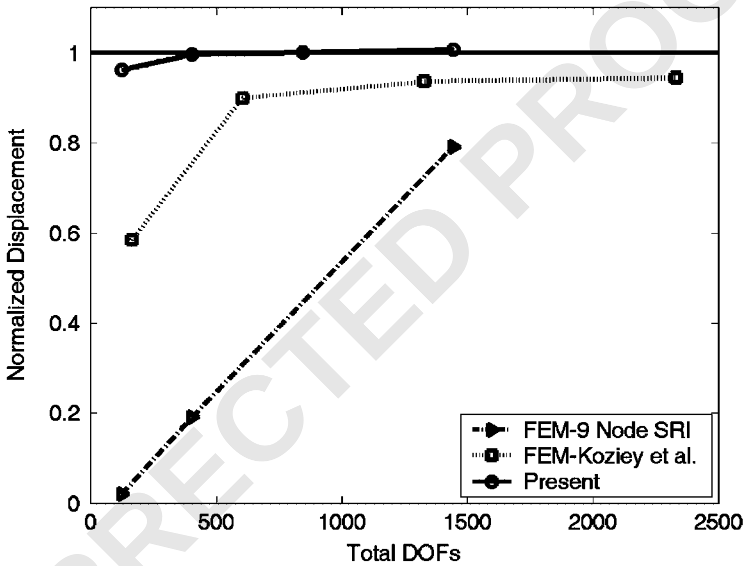

Figure 12. Comparison of the normalized displacement underneath point load in the pinched cylinder with free ends.

modulus $E = 3 \times 10^6$ and Poisson ratio $\nu = 0.3$. The self-equilibrated applied forces are of magnitude $P = 100.0$. The reference solution for the deflection beneath the load is 0.1139 [17]. Due to threefold symmetry, only one-eighth of the cylinder is modelled as shown in Figure 11.

Various discretizations as shown in Figure 11 are used to study the convergence of the numerical solutions. The normalized displacements near the point load location obtained by the proposed method compare very well with the solutions obtained from well-known finite element solutions (9-SRI, References [15, 16]) in Figure 12. The deformed shape is also shown in Figure 13.

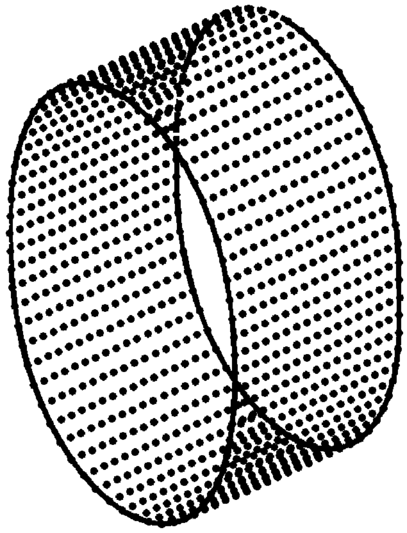

Figure 13. Deformed shape of pinched cylinder with free ends.

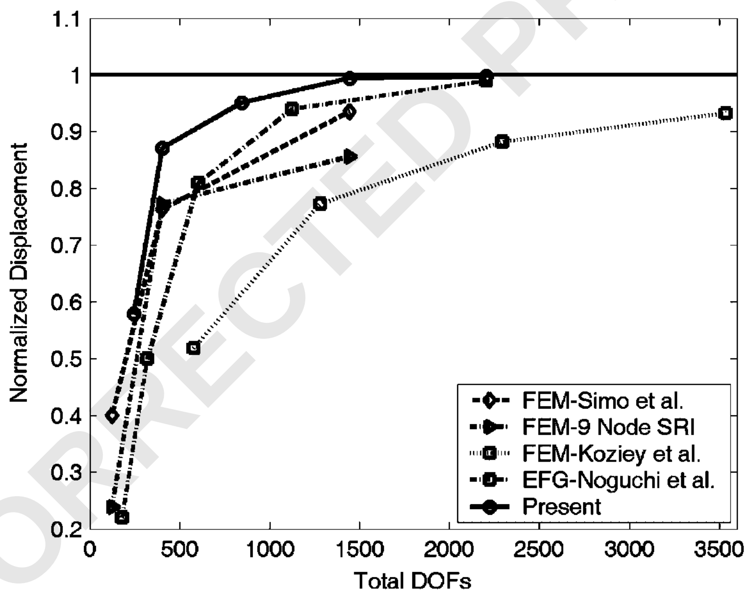

Figure 14. Comparison of the normalized displacement underneath point load in the pinched cylinder with end diaphragms.

1 *6.4. Pinched cylinder with end diaphragms*

This problem is commonly used as a benchmark to test the numerical performance of shell
3 formulations in representing bending, shear, and membrane modes. With reference to Figure 10,

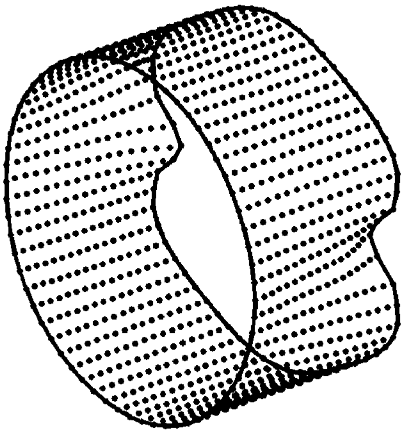

Figure 15. Deformed shape of pinched cylinder with end diaphragms.

the geometry parameters used in this problem are $L = 600$, $R = 300$, and thickness $t = 3$. The material constants are Young's modulus $E = 3 \times 10^6$ and Poisson ratio $\nu = 0.3$. The applied force is $P = 1.0$. The analytical solution of the deflection under the point load is 1.82488×10^{-5} [20].

In Figure 14, the proposed meshfree solution is compared with other finite element solutions obtained using the methods by Simo *et al.* [20], Koziey and Mirza [16]; the nine-node shell element with selective and reduced integration [20], and the element-free Galerkin meshfree shear deformable shell formulation using convected parametric coordinates with bi-cubic basis ($n = 16$) by Noguchi *et al.* [2]. The numerical solutions show that the solution of present method is superior to those obtained from finite element solutions. The deformed geometry predicted by the present method is shown in Figure 15.

7. CONCLUSIONS

In this paper, it has been demonstrated that when imposing the reproducing kernel conditions on discrete nodes located on a constrained geometry (shell surface), the moment matrix associated with the RK shape function becomes singular if the shell surface function is linearly dependent to the basis functions in the RK approximation. To surmount this singularity, two methods have been proposed: dummy node method and pseudo-inverse method. The constrained RK approximation formulated using both methods allows the meshfree shape functions on shell surface be constructed using Cartesian coordinates. This constrained RK approximation is applicable to shell structures with arbitrary geometry, which cannot be done using the standard RK approximation on parametric coordinates. With the proposed constrained RK shape functions, any open or enclosed surface can be represented. It was also shown that consistency conditions in the approximation are approximated within the level of perturbation on shell surface using the constrained RK approximation. An alternative approach is introduced by a pseudo-inverse formulation which eliminates the nullity of the linearly dependent reproducing equations. The resulting RK shape functions constructed by the pseudo-inverse method exactly satisfy reproducing conditions, but the method requires solving eigenvalue problem at every evaluation point and thus consumes higher CPU.

Based on the proposed constrained RK approximation, a meshfree shell formulation in Cartesian coordinates was developed. In this approach, the membrane and shear energy terms were integrated using a direct nodal integration to resolve locking, whereas stabilized nodal integration was used on the bending energy to achieve stability as well as computational efficiency. A curvature smoothing technique on curved shell surface was also introduced in the stabilization of nodal integration. Various numerical examples were analysed, and good performance of present formulation was demonstrated.

ACKNOWLEDGEMENTS

D. Wang gratefully acknowledges the support by the Research Initiation Fund of Xiamen University.

REFERENCES

1. Krysl P, Belytschko T. Analysis of thin shells by the element-free Galerkin method. *International Journal of Solids and Structures* 1996; **33**:3057–3080.
2. Noguchi H, Hawashima T, Miyamura T. Element free analysis of shell and spatial structures. *International Journal for Numerical Methods in Engineering* 2000; **47**:1215–1240.
3. Belytschko T, Lu YY, Gu L. Element-free Galerkin methods. *International Journal for Numerical Methods in Engineering* 1994; **37**:229–256.
4. Belytschko T, Kronggauz Y, Organ D, Fleming M. Meshless methods: an overview and recent developments. *Computer Methods in Applied Mechanics and Engineering* 1996; **139**:3–47.
5. Krysl P, Belytschko T. Analysis of thin plates by the element-free Galerkin method. *Computational Mechanics* 1995; **16**:1–10.
6. Li S, Hao W, Liu WK. Numerical simulations of large deformation of thin shell structures using meshfree method. *Computational Mechanics* 2000; **25**:102–116.
7. Chen JS, Pan C, Wu CT, Liu WK. Reproducing kernel particle methods for large deformation analysis of nonlinear structures. *Computer Methods in Applied Mechanics and Engineering* 1996; **139**:195–227.
8. Liu WK, Jun S, Zhang YF. Reproducing kernel particle methods. *International Journal for Numerical Methods in Fluids* 1995; **20**:1081–1106.
9. Liu WK, Hao W, Chen Y. Multiresolution reproducing kernel particle methods. *Computational Mechanics* 1997; **20**:295–309.
10. Beissel S, Belytschko T. Nodal integration of the element-free Galerkin method. *Computer Methods in Applied Mechanics and Engineering* 1996; **139**:49–74.
11. Chen JS, Wu CT, Yoon S, You Y. A stabilized conforming nodal integration for Galerkin meshfree methods. *International Journal for Numerical Methods in Engineering* 2001; **50**:435–466.
12. Chen JS, Yoon S, Wu CT. Nonlinear version of stabilized conforming nodal integration for Galerkin meshfree methods. *International Journal for Numerical Methods in Engineering* 2002; **53**:2587–2615.
13. Wang D, Chen JS. Locking-free stabilized conforming nodal integration for meshfree Mindlin–Reissner plate formulation. *Computer Methods in Applied Mechanics and Engineering* 2004; **193**:1065–1083.
14. MacNeal, Harder, 1985.
15. Liu WK, Law SE, Lam D, Belytschko T. Resultant stress degenerated shell elements. *Computer Methods in Applied Mechanics and Engineering* 1986; **55**:259–300.
16. Koziey BL, Mirza FA. Consistent thick shell element. *Computers and Structures* 1997; **65**:531–549.
17. Huang HC. *Static and Dynamic Analysis of Plates and Shells*. Springer-Verlag: New York, 1988.
18. Huang HC, Hinton E. A new nine-node degenerated shell element with enhanced membrane and shear interpolation. *International Journal for Numerical Methods in Engineering* 1986; **22**:73–92.
19. Taylor RL. Finite element analysis of linear shell problems. In *Proceedings of the Mathematics of Finite Elements and Applications*, Whiteman SR (ed.). Academic Press: New York, 1987.
20. Simo JC, Fox DD, Rifai MS. On a stress resultant geometrical exact shell model. Part II: The linear theory; computational aspects. *Computer Methods in Applied Mechanics and Engineering* 1989; **73**:53–92.

John Wiley & Sons Ltd
The Atrium, Southern Gate, Chichester West, Sussex PO19 8S

Author Queries For NME 1701

While preparing this paper/manuscript for typesetting, the following queries have arisen

Query No	Proof Page / line no	Details required	Authors Response
1	21/5	'Koziey et al' changed to 'Koziey and Mirza'. Please check if the change is okay.	
2	REF	Please update ref[14],is cited in Section 6.1.	

COPYRIGHT TRANSFER AGREEMENT

Wiley Production No. ....

Re: Manuscript entitled ....

(the "Contribution") written by ....

(the "Contributor") for publication in...

(the "Journal) published by John Wiley & Sons Ltd ("Wiley").

In order to expedite the publishing process and enable Wiley to disseminate your work to the fullest extent, we need to have this Copyright Transfer Agreement signed and returned to us with the submission of your manuscript. If the Contribution is not accepted for publication this Agreement shall be null and void.

A. COPYRIGHT

1. The Contributor assigns to Wiley, during the full term of copyright and any extensions or renewals of that term, all copyright in and to the Contribution, including but not limited to the right to publish, republish, transmit, sell, distribute and otherwise use the Contribution and the material contained therein in electronic and print editions of the Journal and in derivative works throughout the world, in all languages and in all media of expression now known or later developed, and to license or permit others to do so.
2. Reproduction, posting, transmission or other distribution or use of the Contribution or any material contained therein, in any medium as permitted hereunder, requires a citation to the Journal and an appropriate credit to Wiley as Publisher, suitable in form and content as follows: (Title of Article, Author, Journal Title and Volume/Issue Copyright © [year] John Wiley & Sons Ltd or copyright owner as specified in the Journal.)

B. RETAINED RIGHTS

Notwithstanding the above, the Contributor or, if applicable, the Contributor's Employer, retains all proprietary rights other than copyright, such as patent rights, in any process, procedure or article of manufacture described in the Contribution, and the right to make oral presentations of material from the Contribution.

C. OTHER RIGHTS OF CONTRIBUTOR

Wiley grants back to the Contributor the following:

1. The right to share with colleagues print or electronic "preprints" of the unpublished Contribution, in form and content as accepted by Wiley for publication in the Journal. Such preprints may be posted as electronic files on the Contributor's own website for personal or professional use, or on the Contributor's internal university or corporate networks/intranet, or secure external website at the Contributor's institution, but not for commercial sale or for any systematic external distribution by a third party (eg: a listserver or database connected to a public access server). Prior to publication, the Contributor must include the following notice on the preprint: "This is a preprint of an article accepted for publication in [Journal title] Copyright © (year) (copyright owner as specified in the Journal)". After publication of the Contribution by Wiley, the preprint notice should be amended to read as follows: "This is a preprint of an article published in [include the complete citation information for the final version of the Contribution as published in the print edition of the Journal]" and should provide an electronic link to the Journal's WWW site, located at the following Wiley URL: http://www.interscience.wiley.com/. The Contributor agrees not to update the preprint or replace it with the published version of the Contribution.
2. The right, without charge, to photocopy or to transmit on-line or to download, print out and distribute to a colleague a copy of the published Contribution in whole or in part, for the Contributor's personal or professional use, for the advancement of scholarly or scientific research or study, or for corporate informational purposes in accordance with paragraph D2 below.
3. The right to republish, without charge, in print format, all or part of the material from the published Contribution in a book written or edited by the Contributor.
4. The right to use selected figures and tables, and selected text (up to 250 words) from the Contribution, for the Contributor's own teaching purposes, or for incorporation within another work by the Contributor that is made part of an edited work published (in print or electronic format) by a third party, or for presentation in electronic format on an internal computer network or external website of the Contributor or the Contributor's employer. The abstract shall not be included as part of such selected text.
5. The right to include the Contribution in a compilation for classroom use (course packs) to be distributed to students at the Contributor's institution free of charge or to be stored in electronic format in datarooms for access by students at the Contributor's institution as part of their course work (sometimes called "electronic reserve rooms") and for in-house training programmes at the Contributor's employer.

D. CONTRIBUTIONS OWNED BY EMPLOYER

1. If the Contribution was written by the Contributor in the course of the Contributor's employment (as a "work-made-for-hire" in the course of employment), the Contribution is owned by the company/employer which must sign this Agreement (in addition to the Contributor's signature), in the space provided below. In such case, the company/employer hereby assigns to Wiley, during the full term of copyright, all copyright in and to the Contribution for the full term of copyright throughout the world as specified in paragraph A above.
2. In addition to the rights specified as retained in paragraph B above and the rights granted back to the Contributor pursuant to paragraph C above, Wiley hereby grants back, without charge, to such company/employer, its subsidiaries and divisions, the right to make copies of and distribute the published Contribution internally in print format or electronically on the Company's internal network. Upon payment of the Publisher's reprint fee, the institution may distribute (but not re-sell) print copies of the published Contribution externally. Although copies so made shall not be available for individual re-sale, they may be included by the company/employer as part of an information package included with software or other products offered for sale or license. Posting of the published Contribution by the institution on a public access website may only be done with Wiley's written permission, and payment of any applicable fee(s).

E. GOVERNMENT CONTRACTS

In the case of a Contribution prepared under US Government contract or grant, the US Government may reproduce, without charge, all or portions of the Contribution and may authorise others to do so, for official US Government purposes only, if the US Government contract or grant so requires. (Government Employees: see note at end.)

F. COPYRIGHT NOTICE

The Contributor and the company/employer agree that any and all copies of the Contribution or any part thereof distributed or posted by them in print or electronic format as permitted herein will include the notice of copyright as stipulated in the Journal and a full citation to the Journal as published by Wiley.

G. CONTRIBUTOR'S REPRESENTATIONS

The Contributor represents that the Contribution is the Contributor's original work. If the Contribution was prepared jointly, the Contributor agrees to inform the co-Contributors of the terms of this Agreement and to obtain their signature(s) to this Agreement or their written permission to sign on their behalf. The Contribution is submitted only to this Journal and has not been published before, except for "preprints" as permitted above. (If excerpts from copyrighted works owned by third parties are included, the Contributor will obtain written permission from the copyright owners for all uses as set forth in Wiley's permissions form or in the Journal's Instructions for Contributors, and show credit to the sources in the Contribution.) The Contributor also warrants that the Contribution contains no libelous or unlawful statements, does not infringe on the right or privacy of others, or contain material or instructions that might cause harm or injury.

Tick one box and fill in the appropriate section before returning the original signed copy to the Publisher

☐ ***Contributor-owned work***

Contributor's signature .... Date ....

Type or print name and title ....

Co-contributor's signature .... Date ....

Type or print name and title ....

Attach additional signature page as necessary

☐ ***Company/Institution-owned work (made-for-hire in the course of employment)***

Contributor's signature .... Date ....

Type or print name and title ....

Company or Institution
(Employer-for Hire) ....

Authorised signature of Employer .... Date ....

Type or print name and title ....

☐ ***US Government work***

Note to US Government Employees

A Contribution prepared by a US federal government employee as part of the employee's official duties, or which is an official US Government publication is called a "US Government work", and is in the public domain in the United States. In such case, the employee may cross out paragraph A1 but must sign and return this Agreement. If the Contribution was not prepared as part of the employee's duties or is not an official US Government publication, it is not a US Government work.

☐ ***UK Government work (Crown Copyright)***

Note to UK Government Employees

The rights in a Contribution by an employee of a UK Government department, agency or other Crown body as part of his/her official duties, or which is an official government publication, belong to the Crown. In such case, the Publisher will forward the relevant form to the Employee for signature.

WILEY AUTHOR DISCOUNT CARD

As a highly valued contributor to Wiley's publications, we would like to show our appreciation to you by offering a **unique 25% discount** off the published price of any of our books*.

To take advantage of this offer, all you need to do is apply for the **Wiley Author Discount Card** by completing the attached form and returning it to us at the following address:

The Database Group
John Wiley & Sons Ltd
The Atrium
Southern Gate
Chichester
West Sussex PO19 8SQ
UK

In the meantime, whenever you order books direct from us, simply quote promotional code **S001W** to take advantage of the 25% discount.

The newest and quickest way to order your books from us is via our new European website at:

http://www.wileyeurope.com

Key benefits to using the site and ordering online include:

- Real-time SECURE on-line ordering
- The most up-to-date search functionality to make browsing the catalogue easier
- Dedicated Author resource centre
- E-mail a friend
- Easy to use navigation
- Regular special offers
- Sign up for subject orientated e-mail alerts

So take advantage of this great offer, return your completed form today to receive your discount card.

Yours sincerely,

Verity Leaver
E-marketing and Database Manager

*TERMS AND CONDITIONS

This offer is exclusive to Wiley Authors, Editors, Contributors and Editorial Board Members in acquiring books (excluding encyclopaedias and major reference works) for their personal use. There must be no resale through any channel. The offer is subject to stock availability and cannot be applied retrospectively. This entitlement cannot be used in conjunction with any other special offer. Wiley reserves the right to amend the terms of the offer at any time.

REGISTRATION FORM
FOR 25% BOOK DISCOUNT CARD

To enjoy your special discount, tell us your areas of interest and you will receive relevant catalogues or leaflets from which to select your books. Please indicate your specific subject areas below.

Accounting [ ]
- Public [ ]
- Corporate [ ]

Chemistry [ ]
- Analytical [ ]
- Industrial/Safety [ ]
- Organic [ ]
- Inorganic [ ]
- Polymer [ ]
- Spectroscopy [ ]

Encyclopedia/Reference [ ]
- Business/Finance [ ]
- Life Sciences [ ]
- Medical Sciences [ ]
- Physical Sciences [ ]
- Technology [ ]

Earth & Environmental Science [ ]

Hospitality [ ]

Genetics [ ]
- Bioinformatics/Computational [ ]
  Biology [ ]
- Proteomics [ ]
- Genomics [ ]
- Gene Mapping [ ]
- Clinical Genetics [ ]

Medical Science [ ]
- Cardiovascular [ ]
- Diabetes [ ]
- Endocrinology [ ]
- Imaging [ ]
- Obstetrics/Gynaecology [ ]
- Oncology [ ]
- Pharmacology [ ]
- Psychiatry [ ]

Non-Profit [ ]

Architecture [ ]

Business/Management [ ]

Computer Science [ ]
- Database/Data Warehouse [ ]
- Internet Business [ ]
- Networking [ ]
- Programming/Software [ ]
  Development [ ]
- Object Technology [ ]

Engineering [ ]
- Civil [ ]
- Communications Technology [ ]
- Electronic [ ]
- Environmental [ ]
- Industrial [ ]
- Mechanical [ ]

Finance/Investing [ ]
- Economics [ ]
- Institutional [ ]
- Personal Finance [ ]

Life Science [ ]

Landscape Architecture [ ]

Mathematics/Statistics [ ]

Manufacturing [ ]

Material Science [ ]

Psychology [ ]
- Clinical [ ]
- Forensic [ ]
- Social & Personality [ ]
- Health & Sport [ ]
- Cognitive [ ]
- Organizational [ ]
- Developmental and Special Ed [ ]
- Child Welfare [ ]
- Self-Help [ ]

Physics/Physical Science [ ]

[ ] I confirm that I am a Wiley Author/Editor/Contributor/Editorial Board Member of the following publications:

SIGNATURE: ………

PLEASE COMPLETE THE FOLLOWING DETAILS IN BLOCK CAPITALS:

TITLE AND NAME: (e.g. Mr, Mrs, Dr) ……………………………………………………………………………………

JOB TITLE: ………

DEPARTMENT: ………..

COMPANY/INSTITUTION: ……………………………………………………………………………………………………

ADDRESS: ……….

……

……

……

TOWN/CITY: ………

COUNTY/STATE: …….

COUNTRY: ………

POSTCODE/ZIP CODE: ……

DAYTIME TEL: ………

FAX: ………

E-MAIL: ……

YOUR PERSONAL DATA
We, John Wiley & Sons Ltd, will use the information you have provided to fulfil your request. In addition, we would like to:

1. Use your information to keep you informed by post, e-mail or telephone of titles and offers of interest to you and available from us or other Wiley Group companies worldwide, and may supply your details to members of the Wiley Group for this purpose.

   [ ] Please tick the box if you do not wish to receive this information

2. Share your information with other carefully selected companies so that they may contact you by post, fax or e-mail with details of titles and offers that may be of interest to you.

   [ ] Please tick the box if you do not wish to receive this information.

If, at any time, you wish to stop receiving information, please contact the Database Group (databasegroup@wiley.co.uk) at John Wiley & Sons Ltd, The Atrium, Southern Gate, Chichester, West Sussex PO19 8SQ, UK.

E-MAIL ALERTING SERVICE
We offer an information service on our product ranges via e-mail. If you do not wish to receive information and offers from John Wiley companies worldwide via e-mail, please tick the box [ ].

This offer is exclusive to Wiley Authors, Editors, Contributors and Editorial Board Members in acquiring books (excluding encyclopaedias and major reference works) for their personal use. There should be no resale through any channel. The offer is subject to stock availability and may not be applied retrospectively. This entitlement cannot be used in conjunction with any other special offer. Wiley reserves the right to vary the terms of the offer at any time.

Ref: S001W